

Dear Author:

Thank you for publishing with AGU. Your proofs are attached. AGU and Wiley are committed to rapid posting of accepted papers. The accepted version of your paper is already available online (except for embargoed papers), providing visibility, and we strive to have final versions available within a few weeks. Following the guidelines for marking corrections and returning the proofs quickly will allow prompt online posting of the final version of your paper.

AGU Publications recently [updated](#) our style to follow leading practices in scholarly publishing, to simplify corrections and reduce copyediting changes. We are now following the APA style for grammar and markup. This style is used by many other journals and we hope that this change, over time, will lead to a simpler and standard experience for authors.

We have collected some information on how to increase the visibility of your paper [here](#). Many of these steps can be taken after publication, so it is not too late to start. The online version of your paper includes “Altmetrics,” which continually tracks and links to mentions in news outlets, Twitter, blogs, and other social media. A link to articles that cite your paper is also provided. Papers are also linked directly to any highlights provided by AGU and other similar AGU content. Recent highlights across AGU journals are collected [here](#).

AGU is also, through Wiley, working to expand sharing of articles. Wiley piloted an [initiative](#) through the PDF reader Readcube that allows content to be shared freely to colleagues by authors and subscribers. This is now available for AGU content. For authors and subscribers, just click on the “share” link of your article in the Readcube reader. For the public and general reader, this service also allows free access to Wiley and thus AGU content from links in news stories.

Finally, your feedback is important to us. If you have questions or comments regarding your AGU Publications experience, including information on production and proofs, please contact us at publications@agu.org. We will also be contacting you soon after your article is published with an author survey. Please take a few minutes to respond to this online survey; your input is important in improving the overall editorial and production process. Thank you again for supporting AGU.

Sincerely,



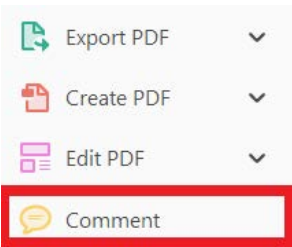
Brooks Hanson
Sr. Vice President, Publications

USING e-ANNOTATION TOOLS FOR ELECTRONIC PROOF CORRECTION


Required software to e-Annotate PDFs: Adobe Acrobat Professional or Adobe Reader (version 11 or above). (Note that this document uses screenshots from Adobe Reader DC.)
The latest version of Acrobat Reader can be downloaded for free at: <http://get.adobe.com/reader/>

Once you have Acrobat Reader open on your computer, click on the [Comment](#) tab (right-hand panel or under the Tools menu).


This will open up a ribbon panel at the top of the document. Using a tool will place a comment in the right-hand panel. The tools you will use for annotating your proof are shown below:

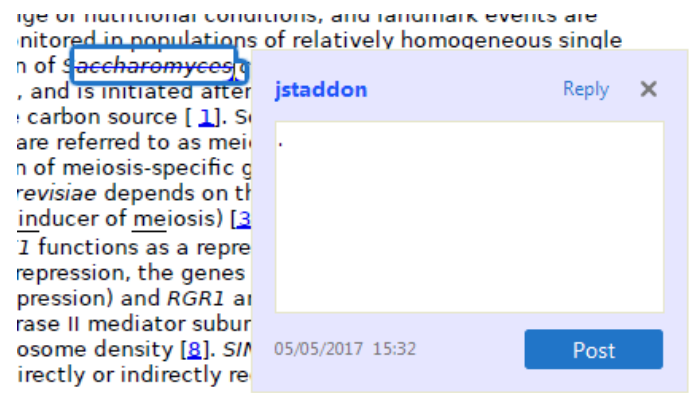


1. **Replace (Ins)** Tool – for replacing text.


 Strikes a line through text and opens up a text box where replacement text can be entered.

How to use it:

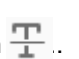
- Highlight a word or sentence.
- Click on .
- Type the replacement text into the blue box that appears.



2. **Strikethrough (Del)** Tool – for deleting text.

 Strikes a red line through text that is to be deleted.



How to use it:

- Highlight a word or sentence.
- Click on .
- The text will be struck out in red.


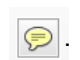
experimental data if available. For ORFs to be had to meet all of the following criteria:

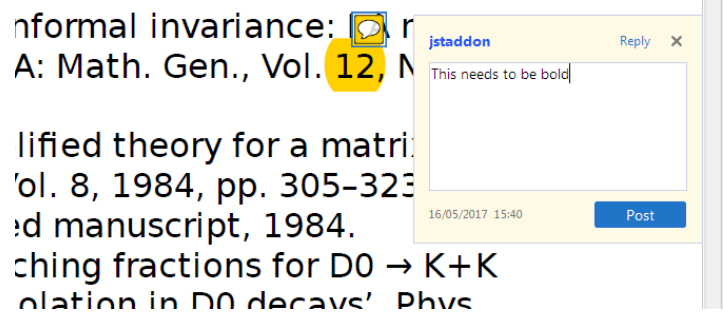
1. Small size (35-250 amino acids).
2. Absence of similarity to known proteins.
3. Absence of functional data which could not be the real overlapping gene.
4. Greater than 25% overlap at the N-terminus with another coding feature; over both ends; or ORF containing a tRNA.

3. **Commenting** Tool – for highlighting a section to be changed to bold or italic or for general comments.


  Use these 2 tools to highlight the text where a comment is then made.

How to use it:


- Click on .
- Click and drag over the text you need to highlight for the comment you will add.
- Click on .
- Click close to the text you just highlighted.
- Type any instructions regarding the text to be altered into the box that appears.

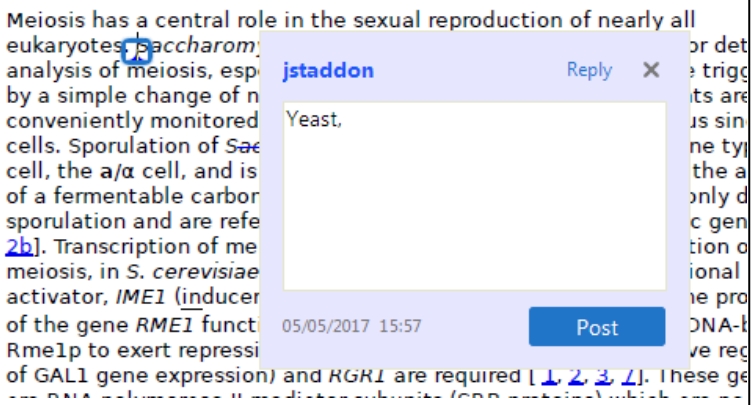


4. **Insert** Tool – for inserting missing text at specific points in the text.


 Marks an insertion point in the text and opens up a text box where comments can be entered.

How to use it:


- Click on .
- Click at the point in the proof where the comment should be inserted.
- Type the comment into the box that appears.



5. **Attach File** Tool – for inserting large amounts of text or replacement figures.

 Inserts an icon linking to the attached file in the appropriate place in the text.


How to use it:

- Click on  .
- Click on the proof to where you'd like the attached file to be linked.
- Select the file to be attached from your computer or network.
- Select the colour and type of icon that will appear in the proof. Click OK.


The attachment appears in the right-hand panel.

chondrial preparator
ative damage injury
e extent of membra
i, malondialdehyde ((TBARS) formation. I
used by high perform

6. **Add stamp** Tool – for approving a proof if no corrections are required.

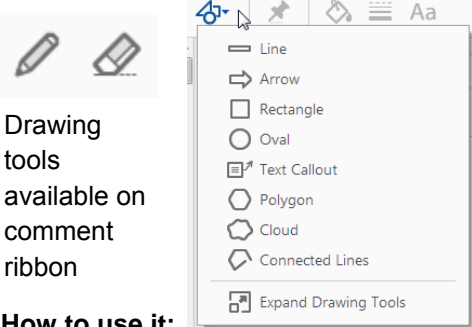
 Inserts a selected stamp onto an appropriate place in the proof.

How to use it:

- Click on  .
- Select the stamp you want to use. (The **Approved** stamp is usually available directly in the menu that appears. Others are shown under *Dynamic*, *Sign Here*, *Standard Business*).
- Fill in any details and then click on the proof where you'd like the stamp to appear. (Where a proof is to be approved as it is, this would normally be on the first page).

of the business cycle, starting with the
on perfect competition, constant ret
production. In this environment goods
extra profits and hence a transfer of market
he market for the good is determined by the model. The New-Key
otaki (1987), has introduced produc
general equilibrium models with nomin
and demand shocks. Most of this literat

APPROVED



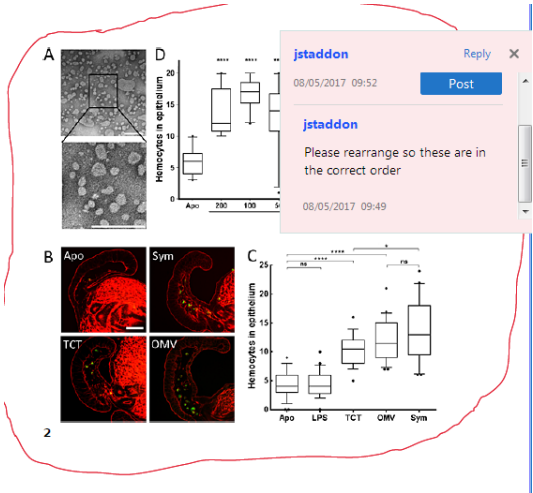
Drawing tools available on comment ribbon

How to use it:

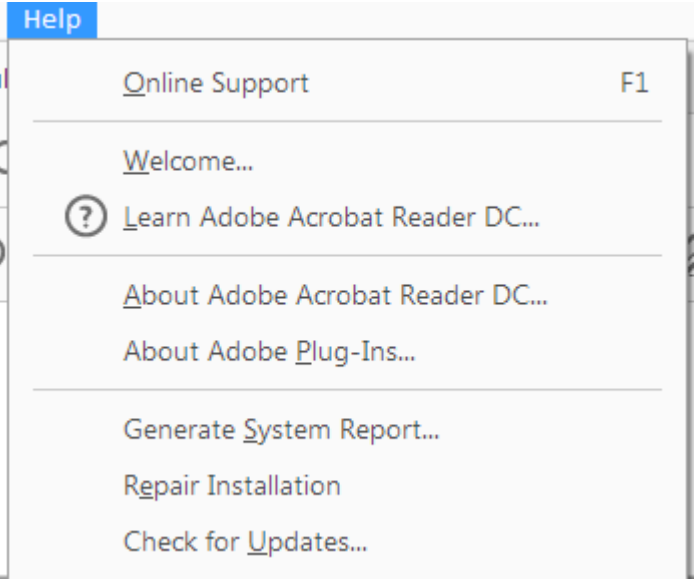
- Click on one of the shapes in the **Drawing Markups** section.
- Click on the proof at the relevant point and draw the selected shape with the cursor.
- To add a comment to the drawn shape, right-click on shape and select *Open Pop-up Note*.
- Type any text in the red box that appears.

7. **Drawing Markups** Tools – for drawing shapes, lines, and freeform annotations on proofs and commenting on these marks.

Allows shapes, lines, and freeform annotations to be drawn on proofs and for comments to be made on these marks.



For further information on how to annotate proofs, click on the **Help** menu to reveal a list of further options:



**PLEASE COMPLETE THE PUBLICATION FEE CONSENT FORM BELOW
AND
RETURN TO THE PRODUCTION EDITOR WITH YOUR PROOF CORRECTIONS**

Please return this completed form and direct any questions to the Wiley Journal Production Editor at GRLprod@wiley.com.

To order OnlineOpen, you must complete the OnlineOpen order form at:

https://authorservices.wiley.com/bauthor/onlineopen_order.asp

Authors who select OnlineOpen will be charged the standard OnlineOpen fee for your journal, but excess publication fees will still apply, if applicable. **If your paper has generated excess publication fees, please complete and return the form below in addition to completing the OnlineOpen order form online (excess fees are billed separately).** If you would like to choose OnlineOpen and you have not already submitted your order online, please do so now.

YOUR ARTICLE DETAILS

Journal: *Geophysical Research Letters*

Article: Shumko, M., Sample, J., Johnson, A., Blake, J.B., Crew, A.B., Spence, H.E., & (2018). Microburst scale size derived from multiple bounces of a microburst simultaneously observed with the FIREBIRD-II CubeSats. *Geophysical Research Letters*, 45, 1–8. <https://doi.org/10.1029/2018GL078925>

OnlineOpen: No **Words:** 3,306 **Tables:** 0 **Figures:** 3 **Total Publishing Units:** 10

Journal Base Fee:		\$500
Excess Publishing Units:	0@\$125	\$0
Publication Fee Total:	USD	\$500

Please provide the information requested below.

Bill to:

Name: _____

Institution: _____

Address: _____

Phone: _____ **Email:** _____

Signature: _____ **Date:** _____

An invoice will be mailed to the address you have provided once your edited article publishes online in its final format. Please include on this publication fee form any information that must be included on the invoice.

Publication Fees and Length Guidelines:

<http://publications.agu.org/author-resource-center/>

Frequently Asked Billing Questions:

[http://onlinelibrary.wiley.com/journal/10.1002/\(ISSN\)2169-8996/homepage/billing_faqs.pdf](http://onlinelibrary.wiley.com/journal/10.1002/(ISSN)2169-8996/homepage/billing_faqs.pdf)

Purchase Order Instructions:

Wiley must be listed as the contractor on purchase orders to prevent delay in processing invoices and payments.

Author Query Form

WILEY

Journal: Geophysical Research Letters

Article: grl57707





Dear Author,

During the copyediting of your manuscript the following queries arose.

Please refer to the query reference call out numbers in the page proofs and respond to each by marking the necessary comments using the PDF annotation tools.

Please remember illegible or unclear comments and corrections may delay publication.

Many thanks for your assistance.

Query No.	Query	Remark
Q1	AUTHOR: Please complete the Publication Fee Consent Form included with your article and return to the Production Editor with your proofs.	
Q2	AUTHOR: Please confirm that given names (Blue) and surnames/family names (Vermilion) have been identified correctly.	They are correct
Q3	AUTHOR: Please verify that the linked ORCID identifiers are correct for each author.	They are correct
Q4	Author: Supporting Information has been supplied with this paper but no citation is provided in the main text of the article. Please provide citation.	
Q5	AUTHOR: Please provide the city location of publisher for Reference Hoots and Roehrich (1980).	
Q6	AUTHOR: Please check that Reference Klumpar et al. (2015) is presented correctly.	
Q7	AUTHOR: Please provide article volume and page range for Reference Mozer, et al. (2018).	

Please confirm that the funding sponsor list below was correctly extracted from your article: that it includes all funders and that the text has been matched to the correct FundRef Registry organization names. If a name was not found in the FundRef registry, it may not be the canonical name form, it may be a program name rather than an organization name, or it may be an organization not yet included in FundRef Registry. If you know of another name form or a parent organization name for a "not found" item on this list below, please share that information.

FundRef name	FundRef Organization Name
National Science Foundation	not found
NASA	not found

RESEARCH LETTER

10.1029/2018GL078925

Key Points:

- Multiple bounces from a microburst were observed by the two FIREBIRD-II Cube-Sats at LEO
- The lower bounds on the microburst scale size at LEO were 29 \pm 1 km (latitudinal) and 51 \pm 11 km (longitudinal)
- Deduced lower bound equatorial scale size was similar to the whistler mode chorus source scale

Supporting Information:

- Supporting Information S1

Correspondence to:

M. Shumko,
msshumko@gmail.com








Citation:

Shumko, M., Sample, J., Johnson, A., Blake, J.B., Crew, A.B., Spence, H.E., & (2018). Microburst scale size derived from multiple bounces of a microburst simultaneously observed with the FIREBIRD-II CubeSats. *Geophysical Research Letters*, 45. <https://doi.org/10.1029/2018GL078925>

Received 25 MAY 2018

Accepted 29 JUN 2018

Microburst Scale Size Derived From Multiple Bounces of a Microburst Simultaneously Observed With the FIREBIRD-II CubeSats

Mykhaylo Shumko¹ , John Sample¹ , Arlo Johnson¹ , Bern Blake² , Alex Crew³ , Harlan Spence⁴ , David Klumpar¹, Oleksiy Agapitov⁵ , and Matthew Handley¹ 

¹Department of Physics, Montana State University, Bozeman, MT, USA, ²Space Science Applications Laboratory, The Aerospace Corporation, Los Angeles, CA, USA, ³The Johns Hopkins University Applied Physics Laboratory LLC, Laurel, MD, USA, ⁴Institute for the Study of Earth, Oceans, and Space, University of New Hampshire, Durham, N.H, USA, ⁵Space Sciences Laboratory, Berkeley, CA, USA



Abstract We present the observation of a spatially large microburst with multiple bounces made simultaneously by the Focused Investigation of Relativistic Electron Bursts: Intensity, Range, and Dynamics II (FIREBIRD-II) CubeSats on 2 February 2015. This is the first observation of a microburst with a subsequent decay made by two coorbiting but spatially separated spacecraft. From these unique measurements, we place estimates on the lower bounds of the spatial scales as well as quantify the electron bounce periods. The microburst's lower bound latitudinal scale size was 29 ± 1 km and the longitudinal scale size was 51 ± 1 km in low Earth orbit. We mapped these scale sizes to the magnetic equator and found that the radial and azimuthal scale sizes were at least 500 ± 10 km and 530 ± 10 km, respectively. These lower bound equatorial scale sizes are similar to whistler mode chorus wave source scale sizes, which supports the hypothesis that microbursts are a product of electron scattering by chorus waves. Lastly, we estimated the bounce periods for 200- to 800-keV electrons and found good agreement with four common magnetic field models.

Plain Language Summary Microbursts are a subsecond impulsive increase of electron precipitation from the outer Van Allen radiation belt into the atmosphere, believed to be an important loss process of radiation belt electrons. Here we present an observation of a microburst observed simultaneously by the twin Focused Investigation of Relativistic Electron Bursts: Intensity, Range, and Dynamics II CubeSats. This unique observation allowed us to calculate the microburst's spatial scale size and electron bounce periods. The spatial scale size in low Earth orbit was found to be a few tens of kilometers in size, one of the largest reported in literature. We then magnetically mapped this scale size to the region near the microburst's generation region and found it to be around 500 km, similar to the spatial scale size of the waves that are believed to be responsible for microburst generation. This observation shows an example of how large microbursts can be, and it sheds light on its scattering mechanism.

1. Introduction

The dynamics of radiation belt electrons are complex and are driven by competition between source and loss processes. A few possible loss processes are radial diffusion (Shprits & Thorne, 2004), magnetopause shadowing (Ukhorskiy et al., 2006), and pitch angle and energy diffusion due to scattering of electrons by plasma waves (e.g., Abel & Thorne, 1998; Horne & Thorne, 2003; Meredith et al., 2002; Mozer et al., 2018; Selesnick et al., 2003; Summers et al., 1998; Thorne et al., 2005). There are a variety of waves that cause pitch angle scattering, including electromagnetic ion cyclotron waves, plasmaspheric hiss, and chorus (Millan & Thorne, 2007; Thorne, 2010). Chorus predominantly occurs in the dawn sector (6–12 magnetic local times, MLT; Li et al., 2009) where it accelerates electrons with large equatorial pitch angles and scatters electrons with small equatorial pitch angles (Horne & Thorne, 2003). Some of these electrons may be impulsively scattered into the loss cone, where they result in short-duration (~ 100 ms) enhancements in precipitating flux called microbursts.

Anderson and Milton (1964) coined the term microburst to describe high-altitude balloon observations of ~ 100 -ms duration enhancements of bremsstrahlung X-rays emitted from scattered microburst electrons

impacting the atmosphere. Since then, nonrelativistic (less than a few hundred keV) microbursts have been routinely observed with other balloon missions (e.g., Anderson et al., 2017; Parks, 1967; Woodger et al., 2015). A review of the literature shows no reports of microbursts above a few hundreds of kiloelectronvolts observed by balloons (Millan et al., 2002; Woodger et al., 2015). This lack of observation may be explained by relatively weaker pitch angle scattering of relativistic electrons by chorus (Lee et al., 2012).

In addition to the X-ray signature for bursts of electron precipitation, the precipitating relativistic and non-relativistic electrons have been measured in situ by spacecraft orbiting in low Earth orbit (LEO). Hereinafter, we refer to these electron signatures observed by LEO spacecraft also as microbursts. Microbursts have been observed with, for example, the Solar Anomalous and Magnetospheric Particle Explorer's (SAMPEX) >150 -keV and >1 -MeV channels (Blake et al., 1996; Blum et al., 2015; Lorentzen, Blake, et al., 2001; Lorentzen, Looper, & Blake, 2001; Nakamura et al., 1995, 2000; O'Brien et al., 2003, 2004) and Focused Investigation of Relativistic Electron Bursts: Intensity, Range, and Dynamics (FIREBIRD-II) with its >200 -keV energy channels (Anderson et al., 2017; Breneman et al., 2017; Crew et al., 2016).

Understanding microburst precipitation and its scattering mechanism is important to radiation belt dynamics. The scattering mechanism has been observationally studied by, for example, Lorentzen, Looper, and Blake (2001) who found that microbursts and chorus waves predominantly occur in the dawn sector and Breneman et al. (2017) made a direct observational link between individual microbursts and chorus elements. Microbursts have been modeled and empirically estimated to be capable of depleting the relativistic electron population in the outer radiation belt on the order of a day (Breneman et al., 2017; O'Brien et al., 2004; Shprits et al., 2007; Thorne et al., 2005). An important parameter in this estimation of instantaneous radiation belt electron losses due to microbursts is their scale size. Parks (1967) used balloon measurements of bremsstrahlung X-rays to estimate the high-altitude scale size of predominantly low-energy microbursts to be 40 ± 14 km. In Blake et al. (1996) a microburst with multiple bounces was observed by SAMPEX, and the microburst's latitudinal scale size in LEO was estimated to have been *at least a few tens of kilometers*. Blake et al. (1996) concluded that typically microbursts are less than a few tens of electron gyroradii in size (at $L = 5$ at LEO, the gyroradii of 1-MeV electrons is on the order of 100 m). Dietrich et al. (2010) used SAMPEX along with ground-based very low frequency stations to conclude that during one SAMPEX pass, the observed microbursts had scale sizes less than 4 km.

Since 1 February 2015, microbursts have been observed by FIREBIRD-II, a pair of CubeSats in LEO. Soon after launch, when the two FIREBIRD-II spacecraft were at close range, a microburst with a scale size greater than 11 km was observed (Crew et al., 2016). On the same day, FIREBIRD-II simultaneously observed a microburst with multiple bounces. The microburst decay was observed over a period of a few seconds, while the spacecraft were traveling predominantly in latitude. Here we present the analysis and results of the latitude and longitude scale sizes and bounce periods of the first microburst with multiple bounces observed with the two FIREBIRD-II spacecraft.

2. Spacecraft and Observation

The FIREBIRD missions are composed of a pair of identically instrumented 1.5U CubeSats ($15 \times 10 \times 10$ cm) that are designed to measure electron precipitation in LEO (Klumpar et al., 2015; Spence et al., 2012). The second mission, termed FIREBIRD-II, was launched on 31 January 2015. The two FIREBIRD-II CubeSats, identified as Flight Unit 3 (FU3) and Flight Unit 4 (FU4), were placed in a 632-km apogee, 433-km perigee, and 99° inclination orbit (Crew et al., 2016). FU3 and FU4 are orbiting in a string of pearls configuration with FU4 ahead, to resolve the space-time ambiguity of microbursts. Each FIREBIRD-II unit has two solid state detectors: one is mounted essentially at the spacecraft surface, covered only by a thin foil acting as a sun shade, with a field of view of 90° (surface detector), and the other is beneath a collimator that restricts the field of view to 54° (collimated detector). Only FU3 has a functioning surface detector, so this analysis utilizes the collimated detectors. FU3's surface and collimated detectors, as well as FU4's collimated detector, observe electron fluxes in six energy channels from ~ 230 keV to >1 MeV. FIREBIRD-II's High-Resolution (HiRes) electron flux data are gathered with an adjustable sampling period of 18.75 ms by default and can be as fast as 12.5 ms.

On 2 February 2015 at 06:12 UT, both FIREBIRD-II spacecraft simultaneously observed an initial microburst, followed by subsequent periodic electron enhancements of diminishing amplitude shown in Figure 1. This is thought to be the signature of a single burst of electrons, some of which precipitate, but the rest mirror near the spacecraft then bounce to the conjugate hemisphere where they mirror again and the subsequent

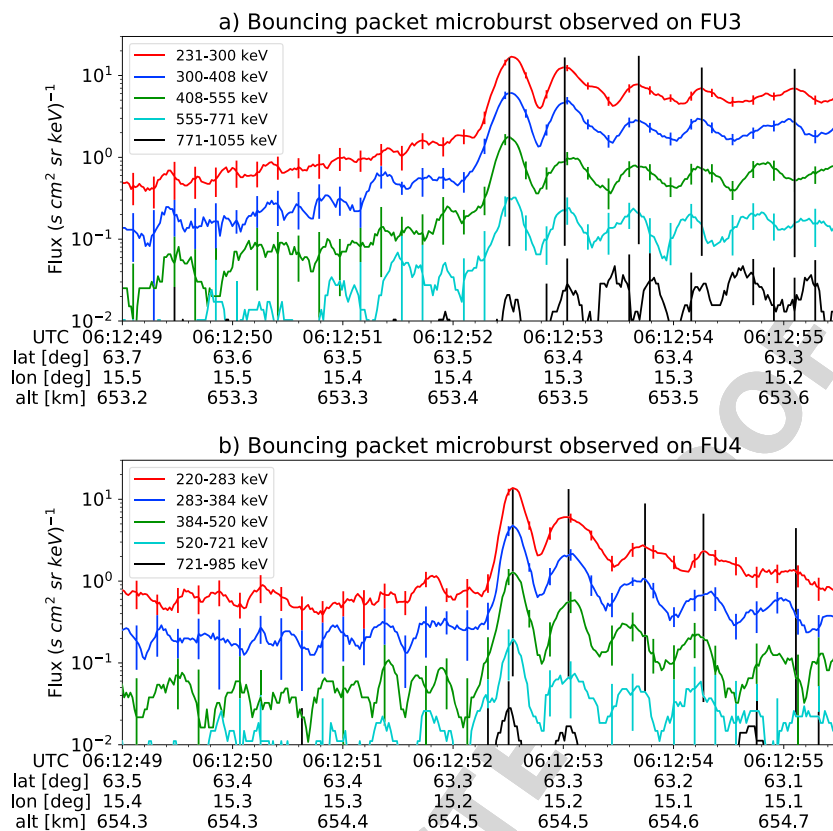


Figure 1. High-resolution data of the microburst observed at 2 February 2015 at 06:12:53 UT, smoothed with a 150-ms rolling average. The subsequent bounces showed some energy dispersion. As discussed in the supporting information, a time correction of -2.28 s was applied to FU3. While the flux from five energy channels is shown, only channels with reasonable counting statistics were used for the spatial scale analysis. Vertical colored bars show the \sqrt{N} error every 10th data point and vertical black bars are lined up with the peaks in the 220- to 283-keV energy channel to help identify dispersion.

bounces produce a train of decaying peaks (Blake et al., 1996; Thorne et al., 2005). This bounce signature occurred during the transition between the main and recovery phases of a storm with a minimum Dst of -44 nT ($Kp = 4$, and $AE \approx 400$ nT). At this time, the HiRes data were sampled at 18.75 ms. Five peaks were observed by both spacecraft. The fifth peak observed by FU4 was comparable to the Poisson noise and was not used in this analysis. This microburst was observed from the first energy channel (≈ 200 – 300 keV), to the fourth energy channel (≈ 500 – 700 keV), and FU3's surface detector observed the microburst up to the fifth energy channel (683 – 950 keV).

The HiRes data in Figure 1 show signs of energy dispersion, characterized by higher-energy electrons arriving earlier than the lower energies. This time of flight energy dispersion tends to smear out the initial sharp burst upon each subsequent bounce. The first peak does not appear to be dispersed, and subsequent peaks show a dispersion trend consistent across energy channels. The black vertical bars have been added to Figure 1 to highlight this energy dispersion. This dispersion signature and amplitude decay implies that the first peak was observed soon after the electrons were scattered, followed by decaying bounces.

At this time, in magnetic coordinates, FIREBIRD-II was at McIlwain $L = 4.7$ and MLT = 8.3, calculated with the Tsyganenko 1989 (T89) magnetic field model (Tsyganenko, 1989) using IRBEM-Lib (Boscher et al., 2012). Geographically, they were above Sweden, latitude = 63° N, longitude = 15° E, altitude = 650 km. This geographic location is magnetically conjugate to the east of the so-called South Atlantic Anomaly (SAA). The SAA is the location where the mirror points of electrons tend to occur at locations deeper in the atmosphere owing to the offset of the dipole magnetic field from the Earth's center. Electrons with pitch angles within the drift loss cone will encounter the SAA and be removed from their eastward longitudinal drift paths (Comess et al., 2013; Dietrich et al., 2010). FU3 and FU4 are therefore both in regions where the particles in the drift

loss cone have recently precipitated, leaving only particles that were recently scattered. At the spacecraft location, locally mirroring electrons would have mirrored at 95 km in the opposite hemisphere, with more field-aligned electrons mirroring at even lower altitudes. From the analysis done by Fang et al. (2010), the peak in the total ionization rate in the atmosphere for 100-keV electrons is around 80-km altitude, while the total ionization rate from 1-MeV electrons peaks around 60-km altitude. It is, therefore, expected that a fraction of the microburst electrons will survive each encounter with the atmosphere. By plotting the peak flux as a function of bounce (not shown), it was found that 40–60% of the microburst electrons were lost on the first bounce, similar to the 33% loss per bounce observed for a bouncing microburst observed by SAMPEX (Thorne et al., 2005).

3. Analysis

At the beginning of the FIREBIRD-II mission, two issues prevented the proper analysis of the microburst's spatial scale size: the spacecraft clocks were not synchronized, and their relative positions were not accurately known. We addressed these issues with a cross-correlation time lag analysis described in detail in the supporting information (SI) (Hoots & Roehrich, 1980). From this analysis, the time correction was 2.28 ± 0.12 s (applied to Figure 1) and the separation was 19.9 ± 0.9 km at the time of the microburst observation.

3.1. Electron Bounce Period

We used this unique observation of bouncing electrons to calculate the bounce period, t_b , as a function of energy and compare it to the energy-dependent t_b curves derived from four magnetic field models, the results of which are shown in Figure 2. The observed t_b and uncertainties were calculated by fitting the baseline-subtracted HiRes flux. The baseline flux used in this analysis is given in O'Brien et al. (2004) as the flux at the 10th percentile over a specified time interval, which in this analysis was taken to be 0.5 s. The flux was fitted with a superposition of Gaussians for each energy channel, and the uncertainty in flux was calculated using the Poisson error from the microburst and baseline fluxes summed in quadrature. Using the fit parameters, the mean t_b for the lowest four energy channels is shown in Figure 2. The trend of decreasing t_b as a function of energy is evident in Figure 2, which further supports the assumption that the subsequent peaks are bounces, and not a train of microbursts scattered by bouncing chorus.

The decaying peaks in the 231- to 408-keV electron flux observed by FU3's lowest two energy channels (see Figure 1) were right skewed. One explanation is that there was in-channel energy dispersion within those channels. Since t_b of higher-energy electrons is shorter, a right-skewed peak implies that higher-energy electrons were more abundant within that channel, for example, in FU3's 231- to 300-keV channel, the 300-keV electrons will arrive sooner than the 231-keV electrons, but will they will be binned in the same channel. A Gaussian fit cannot account for this in-channel dispersion, and as a first-order correction, minima between peaks were used to calculate t_b and are shown in Figure 2. The observed energy-dependent dispersion shown in Figure 2 is consistent with higher-energy peaks returning sooner. This dispersion consistency further supports the assumption that the subsequent peaks are bounces, and not a train of microbursts scattered by bouncing chorus.

To compare the observed and modeled t_b , we superposed t_b curves for various models including an analytical solution in a dipole (Schulz & Lanzerotti, 1974), and numerical models: T89, Tsyganenko 2004 (T04; Tsyganenko & Sitnov, 2005), and Olson and Pfizter Quiet (Olson & Pfizter, 1982) in Figure 2. The numerical t_b curves were calculated using a wrapper for IRBEM-Lib. This code traces the magnetic field line between mirror points and calculates t_b assuming conservation of energy and the first adiabatic invariant for electrons mirroring at FIREBIRD-II. With the empirical t_b , the models agree within FIREBIRD-II's uncertainties, but the T04 model has the largest discrepancy compared to the other models.

3.2. Microburst Energy Spectra

Next, we investigated the energy spectra of this microburst. The energy spectra were modeled with an exponential that was fit to the peak flux derived from the Gaussian fit parameters in section 3.1 to all but the highest energy channel. We found that the e -folding energy, $E_0 \sim 100$ keV. These spectra are similar to spectra showed by Lee et al. (2005) from STSAT-1 and Datta et al. (1997) from sounding rocket measurements. The energy spectra are soft for a typical microburst observed with FIREBIRD-II, and there was no statistically significant change in E_0 for subsequent bounces.

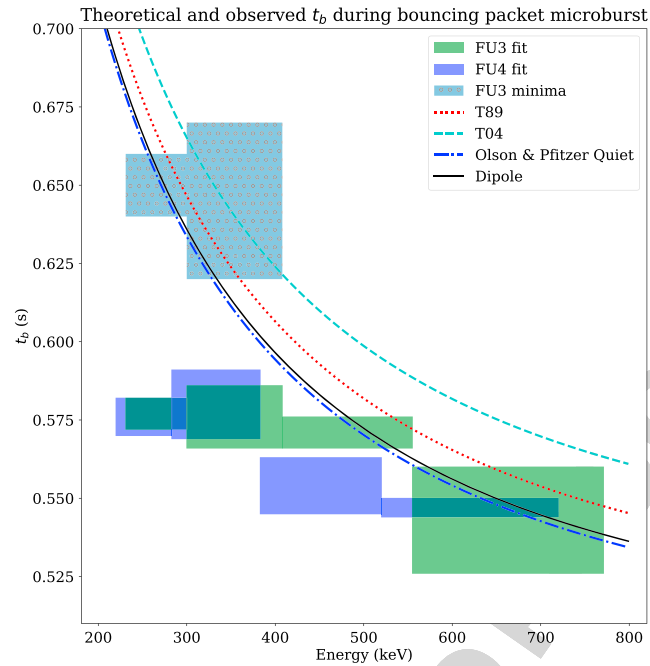


Figure 2. Observed and theoretical t_b for electrons of energies from 200 to 770 keV. The solid black line is t_b in a dipole magnetic field, derived in Schulz and Lanzerotti (1974). The red dotted and cyan dashed lines are the t_b derived using the T89, and T04 magnetic field models with IRBEM-Lib. Lastly, the blue dot-dash curve is the t_b derived using the Olson and Pfizter Quiet model. The green and purple rectangles represent the observed t_b for Flight Unit 3 (FU3) and Flight Unit 4 (FU4) using a Gaussian fit, respectively. The blue rectangles represent the observed t_b calculated with the minima between the bounces. The width of the boxes represent the width of those energy channels, and the height represents the uncertainty from the fit.

3.3. Microburst Scale Sizes

Lastly, after we applied the time and separation corrections detailed in the SI, we mapped the locations of FU3 and FU4 in Figure 3. The locations where FU3 saw peaks 1–5 and where FU4 saw peaks 1–4 are shown as P1–5 and P1–4, respectively. The lower bound on the latitudinal extent of the microburst was the difference in latitude between P1 on FU3 and P4 on FU4 and was found to be 29 ± 1 km. The uncertainty was estimated from the spacecraft separation uncertainty described in the SI. This scale size is the largest reported by FIREBIRD-II.

In section 3.1, we showed that the observed decaying peaks were likely due to bouncing, so we assume that the observed electrons in subsequent bounces were the drifted electrons from the initial microburst. Under this assumption, the scattered electrons observed in the last bounce by FIREBIRD-II must have drifted east from their initial scattering longitude, allowing us to calculate the minimum longitudinal scale size. Following geometrical arguments, the distance that electrons drift east in a single bounce is a product of the circumference of the drift shell foot print, and the fraction of the total drift orbit traversed in a single bounce and is given by

$$d_{az} = 2\pi(R_E + A) \cos(\lambda) \frac{t_b}{\langle T_d \rangle} \quad (1)$$

where R_E is the Earth's radius, A is the spacecraft altitude, λ is the magnetic latitude, t_b is the electron bounce period, and $\langle T_d \rangle$ is the electron drift period. Parks (2003) derived $\langle T_d \rangle$ to be,

$$\langle T_d \rangle \approx \begin{cases} 43.8/(L \cdot E) & \text{if } \alpha_0 = 90^\circ \\ 62.7/(L \cdot E) & \text{if } \alpha_0 = 0^\circ \end{cases} \quad (2)$$

where E is the electron energy in MeV, L is the L shell, and α_0 is the equatorial pitch angle. Electrons mirroring at FIREBIRD-II have $\alpha_0 \approx 3.7^\circ$ and so the $\alpha_0 = 0^\circ$ limit was used.

The microburst's longitudinal scale size is defined as the distance the highest energy electrons drifted in the time between the observations of the first and last peaks. This scale size is given by $D_{az} = n d_{az}$ where n is the

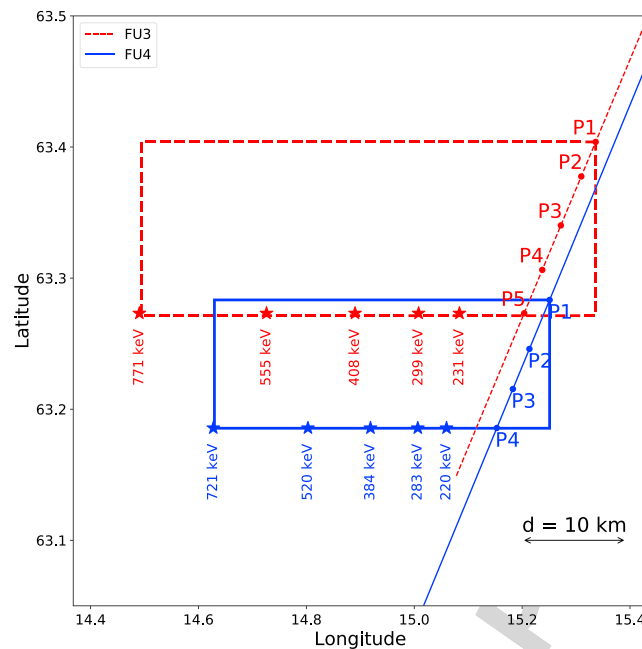


Figure 3. The topology of the FIREBIRD-II orbit and the multiple bounces of the microburst projected onto latitude and longitude with axis scaled to equal distance. Attributes relating to FU3 shown in red dashed lines, and FU4 with blue solid lines. The spacecraft path is shown with the diagonal lines, starting at the upper right corner. The labels P1–4 for FU4 and P1–5 for FU3 indicate where the spacecraft were when the N^{th} peak was seen in the lowest energy channel in the High-resolution data. The stars with the accompanying energy labels represent the locations of the electrons with that energy that started at time of P1 and were seen at the last peak on each spacecraft. The rectangles represent the lower bound of the microburst scale size, assuming that the majority of the electrons were in the upper boundary of energy channel 4.

number of bounces observed. The stars in Figure 3 (with labels corresponding to energy channel boundaries) represent the locations when the microburst was observed at P1, such that an electron of that energy would drift eastward to be seen at P5 for FU3 and P4 for FU4. Since FU3 observed more peaks it observed the larger longitudinal scale size which is shown with the red dashed box in Figure 3. FU3's fourth energy channel's bounds are 555 and 771 keV, which correspond to longitudinal distances of 39 ± 1 km and 51 ± 1 , respectively. The uncertainty was estimated by propagating the uncertainty in the bounce time equation (1). While the observed minimum longitudinal scale size is dependent on FIREBIRD-II's energy channels, the true scale size may not be.

To investigate how the microburst scale size compares to the scale sizes of chorus waves near the magnetic equator, the microburst's longitudinal and latitudinal scale sizes and their uncertainties in LEO were mapped to the magnetic equator with T89. The radial scale size (latitudinal scale mapped from LEO) was greater than 500 ± 10 km. The azimuthal scale size (longitudinal scale mapped from LEO) of 555-keV electrons was greater than 450 ± 10 km, and for the 771-keV electrons it was greater than 530 ± 10 km. The lower bound microburst scale size is similar to the chorus scale sizes derived by Agapitov et al., (2011, 2017) and is discussed below.

4. Discussion and Conclusions

We presented the first observation of a large microburst with multiple bounces made possible by the twin FIREBIRD-II CubeSats. The microburst's lower bound LEO latitudinal and longitudinal scale sizes of 29 ± 1 km and 51 ± 1 km make it one of the largest observed. The microburst's LEO scale size was larger than the latitudinal scale sizes of typical >1 -MeV microbursts reported in Blake et al. (1996), approximately 10 times larger than reported in Dietrich et al. (2010), and approximately 2.6 times larger than other simultaneous microbursts observed by FIREBIRD-II (Crew et al., 2016). Lastly, the scale sizes derived here were similar to the scale sizes of >15 -keV microbursts observed with a high-altitude balloon (Parks, 1967). No energy dependence on the minimum latitudinal scale size was observed, while the observed energy dependence of the minimum longitudinal scale size is an artifact of the technique we used to estimate their drift motion.

The microburst scale size obtained in section 3.3 and scaled to the geomagnetic equator can be compared with the scales of chorus waves presumably responsible for the rapid burst electron precipitation. Early direct estimates of the chorus source scales were made by the coordinated measurement by ISEE-1, 2. The wave power correlation scale was estimated to be about several hundred kilometers across the background magnetic field (Gurnett et al., 1979). Furthermore, Santolik et al. (2003) determined the correlation lengths of chorus-type whistler waves to be around 100 km based on multipoint CLUSTER Wide Band Data measurements near the chorus source region at $L \approx 4$, during the magnetic storm of 18 April 2002. Agapitov et al., (2017, 2011, 2010) recently showed that the spatial extent of chorus source region can be larger, ranging from 600 km in the outer radiation belt to more than 1,000 km in the outer magnetosphere. The lower bound azimuthal and latitudinal scales obtained in section 3.3 and scaled to the magnetic equator are similar to the whistler mode chorus source scale sizes reported in Agapitov et al., (2017, 2011).

No wave measurements from nearby spacecraft were available at this time. Nevertheless, during the hours before and after this observation, the Van Allen Probes' (Mauk et al., 2013) Electric and Magnetic Field Instrument and Integrated Science (Kletzing et al., 2013) observed strong wave power in the lower band chorus frequency range, inside the outer radiation belt between 22 and 2 MLT. Furthermore, $AE \sim 400$ nT at this time, and relatively strong chorus waves were statistically more likely to be present at FIREBIRD-II's MLT (Li et al., 2009).

The empirically estimated and modeled t_b in this study agree within FIREBIRD-II's uncertainties, confirming that the energy-dependent dispersion was due to bouncing. The t_b curves are a proxy for field line length, and this agreement implies that they are comparable. This is expected since the magnetosphere is not drastically compressed at 8 MLT, but we expect a larger discrepancy near midnight, where the magnetosphere is more stretched and difficult to accurately model. In future studies, this analysis can be used as a diagnostic tool to validate field line lengths and improve magnetic field models.

The similarity of the microburst and chorus source region scale sizes, as well as magnetospheric location and conditions, further supports the causal relationship between microbursts and chorus.

Acknowledgments

This work was made possible with help from the FIREBIRD team, and the members of the Space Sciences and Engineering Laboratory at Montana State University for their hard work to make this mission a success. In addition, M. Shumko acknowledges Drew Turner for his suggestions regarding the bounce period calculations, and Dana Longcope for his proofreading feedback. The FIREBIRD-II data are available at http://solar.physics.montana.edu/FIREBIRD_II/. This analysis is supported by the National Science Foundation under grants 0838034 and 1339414. Furthermore, the work of O. Agapitov was supported by the NASA grant NNX16AF85G.

References

- Abel, B., & Thorne, R. M. (1998). Electron scattering loss in Earth's inner magnetosphere: 1. Dominant physical processes. *Journal of Geophysical Research: Space Physics*, 103(A2), 2385–2396.
- Agapitov, O., Blum, L. W., Mozer, F. S., Bonnell, J. W., & Wygant, J. (2017). Chorus whistler wave source scales as determined from multipoint Van Allen Probe measurements, 44, 2634–2642. <https://doi.org/10.1002/2017GL072701>
- Agapitov, O., Krasnoselskikh, V., Dudok de Wit, T., Khotyaintsev, Y., Pickett, J. S., Santolik, O., & Rolland, G. (2011). Multispacecraft observations of chorus emissions as a tool for the plasma density fluctuations' remote sensing. *Journal of Geophysical Research: Space Physics*, 116, A09222. <https://doi.org/10.1029/2011JA016540>
- Agapitov, O., Krasnoselskikh, V., Zaliznyak, Y., Angelopoulos, V., Le Contel, O., & Rolland, G. (2010). Chorus source region localization in the Earth's outer magnetosphere using THEMIS measurements. *Annales Geophysicae*, 28(6), 1377–1386. <https://doi.org/10.5194/angeo-28-1377-2010>
- Anderson, K. A., & Milton, D. W. (1964). Balloon observations of X rays in the auroral zone: 3. High time resolution studies. *Journal of Geophysical Research: Space Physics*, 69(21), 4457–4479. <https://doi.org/10.1029/JZ069i021p04457>
- Anderson, B., Shekhar, S., Millan, R., Crew, A., Spence, H., Klumpar, D., et al. (2017). Spatial scale and duration of one microburst region on 13 August 2015. *Journal of Geophysical Research: Space Physics*, 122, 5949–5964.
- Blake, J., Looper, M., Baker, D., Nakamura, R., Klecker, B., & Hovestadt, D. (1996). New high temporal and spatial resolution measurements by SAMPEX of the precipitation of relativistic electrons. *Advances in Space Research*, 18(8), 171–186. [https://doi.org/10.1016/0273-1177\(95\)00969-8](https://doi.org/10.1016/0273-1177(95)00969-8)
- Blum, L., Li, X., & Denton, M. (2015). Rapid MeV electron precipitation as observed by SAMPEX/HILT during high-speed stream-driven storms. *Journal of Geophysical Research: Space Physics*, 120, 3783–3794. <https://doi.org/10.1002/2014JA020633>
- Boscher, D., Bourdarie, S., O'Brien, P., Guild, T., & Shumko, M. (2012). IRBEM-LIB library.
- Breneman, A., Crew, A., Sample, J., Klumpar, D., Johnson, A., Agapitov, O., et al. (2017). Observations directly linking relativistic electron microbursts to whistler mode chorus: Van Allen Probes and FIREBIRD II. *Geophysical Research Letters*, 44, 11,265–11,272.
- Comess, M., Smith, D., Selesnick, R., Millan, R., & Sample, J. (2013). Dusk-side relativistic electron precipitation as measured by SAMPEX: A statistical survey. *Journal of Geophysical Research: Space Physics*, 118, 5050–5058. <https://doi.org/10.1002/jgra.50481>
- Crew, A. B., Spence, H. E., Blake, J. B., Klumpar, D. M., Larsen, B. A., O'Brien, T. P., et al. (2016). First multipoint in situ observations of electron microbursts: Initial results from the NSF FIREBIRD II mission. *Journal of Geophysical Research: Space Physics*, 121, 5272–5283. <https://doi.org/10.1002/2016JA022485>
- Datta, S., Skoug, R., McCarthy, M., & Parks, G. (1997). Modeling of microburst electron precipitation using pitch angle diffusion theory. *Journal of Geophysical Research: Space Physics*, 102(A8), 17,325–17,333.
- Dietrich, S., Rodger, C. J., Clilverd, M. A., Bortnik, J., & Raita, T. (2010). Relativistic microburst storm characteristics: Combined satellite and ground-based observations. *Journal of Geophysical Research: Space Physics*, 115, A12240.
- Fang, X., Randall, C. E., Lummerzheim, D., Wang, W., Lu, G., Solomon, S. C., & Frahm, R. A. (2010). Parameterization of monoenergetic electron impact ionization. *Geophysical Research Letters*, 37, L22106.
- Gurnett, D., Anderson, R., Scarf, F., Fredricks, R., & Smith, E. (1979). Initial results from the ISEE-1 and-2 plasma wave investigation. *Space Science Reviews*, 23(1), 103–122.

- Hoots, F. R., & Roehrich, R. L. (1980). Models for propagation of norad element sets (*Tech. Rep. 3*): Spacetrack.
- Horne, R. B., & Thorne, R. M. (2003). Relativistic electron acceleration and precipitation during resonant interactions with whistler-mode chorus. *Geophysical Research Letters*, 30(10), 1527. <https://doi.org/10.1029/2003GL016973>
- Kletzing, C., Kurth, W., Acuna, M., MacDowall, R., Torbert, R., Averkamp, T., et al. (2013). The electric and magnetic field instrument suite and integrated science (EMFISIS) on RBSP. *Space Science Reviews*, 179(1-4), 127–181.
- Klumpar, D., Springer, L., Mosleh, E., Mashburn, K., Berardinelli, S., Gunderson, A., et al. (2015). Flight system technologies enabling the twin-CubeSat FIREBIRD II scientific mission. In *Proceedings of the 29th Annual AIAA/USU Conference on Small Satellites*, Logan, Utah, USA.
- Lee, J. J., Parks, G. K., Lee, E., Tsurutani, B. T., Hwang, J., Cho, K. S., et al. (2012). Anisotropic pitch angle distribution of 100 keV microburst electrons in the loss cone: Measurements from STSAT-1. *Annales Geophysicae*, 30(11), 1567–1573. <https://doi.org/10.5194/angeo-30-1567-2012>
- Lee, J.-J., Parks, G. K., Min, K. W., Kim, H. J., Park, J., Hwang, J., et al. (2005). Energy spectra of 170–360 keV electron microbursts measured by the Korean STSAT-1. *Geophysical Research Letters*, 32, 113106. <https://doi.org/10.1029/2005GL022996>
- Li, W., Thorne, R. M., Angelopoulos, V., Bortnik, J., Cully, C. M., Ni, B., et al. (2009). Global distribution of whistler-mode chorus waves observed on the THEMIS spacecraft. *Geophysical Research Letters*, 36, 109104. <https://doi.org/10.1029/2009GL037595>
- Lorentzen, K. R., Blake, J. B., Inan, U. S., & Bortnik, J. (2001). Observations of relativistic electron microbursts in association with VLF chorus. *Journal of Geophysical Research: Space Physics*, 106(A4), 6017–6027. DOI 10.1029/2000JA003018.
- Lorentzen, K. R., Looper, M. D., & Blake, J. B. (2001). Relativistic electron microbursts during the GEM storms. *Geophysical Research Letters*, 28(13), 2573–2576. <https://doi.org/10.1029/2001GL012926>
- Mauk, B., Fox, N. J., Kanekal, S., Kessel, R., Sibeck, D., & Ukhorskiy, A. (2013). Science objectives and rationale for the Radiation Belt Storm Probes mission. *Space Science Reviews*, 179(1-4), 3–27.
- Meredith, N., Horne, R., Summers, D., Thorne, R., Iles, R., Heynderickx, D., & Anderson, R. (2002). Evidence for acceleration of outer zone electrons to relativistic energies by whistler mode chorus. *Annales Geophysicae*, 20, 967–979.
- Millan, R. M., Lin, R., Smith, D., Lorentzen, K., & McCarthy, M. (2002). X-ray observations of MeV electron precipitation with a balloon-borne germanium spectrometer. *Geophysical Research Letters*, 29(24), 47–147-4.
- Millan, R., & Thorne, R. (2007). Review of radiation belt relativistic electron losses. *Journal of Atmospheric and Solar-Terrestrial Physics*, 69(3), 362–377. <https://doi.org/10.1016/j.jastp.2006.06.019>, Global Aspects of Magnetosphere-Ionosphere Coupling Global Aspects of Magnetosphere-Ionosphere Coupling.
- Mozer, F. S., Agapitov, O. V., Blake, J. B., & Vasko, I. Y. (2018). Simultaneous observations of lower band chorus emissions at the equator and microburst precipitating electrons in the ionosphere. *Geophysical Research Letters*. <https://doi.org/10.1002/2017GL076120>
- Nakamura, R., Baker, D. N., Blake, J. B., Kanekal, S., Klecker, B., & Hovestadt, D. (1995). Relativistic electron precipitation enhancements near the outer edge of the radiation belt. *Geophysical Research Letters*, 22(9), 1129–1132. <https://doi.org/10.1029/95GL00378>
- Nakamura, R., Isowa, M., Kamide, Y., Baker, D., Blake, J., & Looper, M. (2000). Observations of relativistic electron microbursts in association with VLF chorus. *Journal of Geophysical Research*, 105, 15,875–15,885.
- O'Brien, T. P., Looper, M. D., & Blake, J. B. (2004). Quantification of relativistic electron microburst losses during the GEM storms. *Geophysical Research Letters*, 31, 104802. <https://doi.org/10.1029/2003GL018621>
- O'Brien, T. P., Lorentzen, K. R., Mann, I. R., Meredith, N. P., Blake, J. B., Fennell, J. F., et al. (2003). Energization of relativistic electrons in the presence of ULF power and MeV microbursts: Evidence for dual ULF and VLF acceleration. *Journal of Geophysical Research: Space Physics*, 108(A8), 1329. <https://doi.org/10.1029/2002JA009784>
- Olson, W. P., & Pfitzer, K. A. (1982). A dynamic model of the magnetospheric magnetic and electric fields for July 29, 1977. *Journal of Geophysical Research: Space Physics*, 87(A8), 5943–5948. <https://doi.org/10.1029/JA087iA08p05943>
- Parks, G. K. (1967). Spatial characteristics of auroral-zone X-ray microbursts. *Journal of Geophysical Research: Space Physics*, 72(1), 215–226.
- Parks, G. (2003). *Physics of space plasmas: An introduction* (Second Edition). Boulder, Colorado: Westview Press.
- Santolík, O., Gurnett, D., Pickett, J., Parrot, M., & Cornilleau-Wehrlin, N. (2003). Spatio-temporal structure of storm-time chorus. *Journal of Geophysical Research: Space Physics*, 108(A7), 1278.
- Schulz, M., & Lanzerotti, L. J. (1974). *Particle diffusion in the radiation belts*. Berlin: Springer.
- Selesnick, R. S., Blake, J. B., & Mewaldt, R. A. (2003). Atmospheric losses of radiation belt electrons. *Journal of Geophysical Research: Space Physics*, 108(A12), 1468. <https://doi.org/10.1029/2003JA010160>
- Shprits, Y. Y., Meredith, N. P., & Thorne, R. M. (2007). Parameterization of radiation belt electron loss timescales due to interactions with chorus waves. *Geophysical Research Letters*, 34, 111110. <https://doi.org/10.1029/2006GL029050>
- Shprits, Y. Y., & Thorne, R. M. (2004). Time dependent radial diffusion modeling of relativistic electrons with realistic loss rates. *Geophysical Research Letters*, 31, 108805. <https://doi.org/10.1029/2004GL019591>
- Spence, H. E., Blake, J. B., Crew, A. B., Driscoll, S., Klumpar, D. M., Larsen, B. A., et al. (2012). Focusing on size and energy dependence of electron microbursts from the Van Allen radiation belts. *Space Weather*, 10, S11004. <https://doi.org/10.1029/2012SW000869>
- Summers, D., Thorne, R. M., & Xiao, F. (1998). Relativistic theory of wave-particle resonant diffusion with application to electron acceleration in the magnetosphere. *Journal of Geophysical Research: Space Physics*, 103(A9), 20,487–20,500.
- Thorne, R. M. (2010). Radiation belt dynamics: The importance of wave-particle interactions. *Geophysical Research Letters*, 37, 122107. <https://doi.org/10.1029/2010GL044990>
- Thorne, R. M., O'Brien, T. P., Shprits, Y. Y., Summers, D., & Horne, R. B. (2005). Timescale for MeV electron microburst loss during geomagnetic storms. *Journal of Geophysical Research: Space Physics*, 110, a09202. <https://doi.org/10.1029/2004JA010882>
- Tsyganenko, N. (1989). A solution of the Chapman-Ferraro problem for an ellipsoidal magnetopause. *Planetary and Space Science*, 37(9), 1037–1046. [https://doi.org/10.1016/0032-0633\(89\)90076-7](https://doi.org/10.1016/0032-0633(89)90076-7)
- Tsyganenko, N. A., & Sitnov, M. I. (2005). Modeling the dynamics of the inner magnetosphere during strong geomagnetic storms. *Journal of Geophysical Research: Space Physics*, 110, a03208. <https://doi.org/10.1029/2004JA010798>
- Ukhorskiy, A. Y., Anderson, B. J., Brandt, P. C., & Tsyganenko, N. A. (2006). Storm time evolution of the outer radiation belt: Transport and losses. *Journal of Geophysical Research: Space Physics*, 111, a11503. <https://doi.org/10.1029/2006JA011690>
- Woodger, L., Halford, A., Millan, R., McCarthy, M., Smith, D., Bowers, G., et al. (2015). A summary of the barrel campaigns: Technique for studying electron precipitation. *Journal of Geophysical Research: Space Physics*, 120(6), 4922–4935.